ISSN 1819-7140, Russian Journal of Pacific Geology, 2016, Vol. 10, No. 4, pp. 299–316. © Pleiades Publishing, Ltd., 2016.
Original Russian Text © S.A. Medvedeva, 2016, published in Tikhookeanskaya Geologiya, 2016, Vol. 35, No. 4, pp. 65–82.

New Data on Chemical Composition of Jurassic–Lower Cretaceous Sedimentary Rocks of the Bureya Basin (Far East of Russia)

S. A. Medvedeva

Kosygin Institute of Tectonics and Geophysics, Far East Branch, Russian Academy of Sciences, ul. Kim Yu Chena 65, Khabarovsk, 680000 Russia

e-mail: medvedeva@itig.as.khb.ru

Received March 20, 2015

Abstract—The first data on the whole-rock chemical composition of Jurassic–Lower Cretaceous sedimentary rocks cropping out in the Soloni–Umal'ta river interfluve (Bureya sedimentary basin) are used for revealing the distribution of their rock-forming elements. It is shown that the clastic material originated mostly from acid igneous rocks, while their intermediate varieties, as well as quartz-rich sedimentary and metamorphic rocks, played a subordinate role. It is assumed that the bulk of the clastic material was transported from the west and southwest (Bureya massif) and a smaller share from the east. The most significant differences between the Lower–Middle Jurassic and Upper Jurassic–Lower Cretaceous rocks mark a break in sedimentation.

Keywords: sandstones, clayey–aleuropelitic rocks, lithochemistry, Jurassic, Cretaceous, Bureya sedimentary basin, Far East of Russia

DOI: 10.1134/S1819714016040060

INTRODUCTION

The original factual data on the whole-rock chemical composition of the Jurassic–Lower Cretaceous sedimentary rocks in the Bureya sedimentary basin served as a basis for this investigation. Its main purpose was to reveal the lithogeochemical features of these rocks and determine, based on their analysis, the composition and location of the main sources of clastic material.

The Bureya basin hosts hard coal and gas deposits with insufficiently known reserves. With further study, more extensive reserves and oil deposits may be discovered. Prospecting and exploration works in the area have been accompanied by variably detailed geological–geophysical (including special) investigations, most of which were dedicated to the study of the Upper Jurassic and Cretaceous rocks of the productive coralliferous sequence [2, 5, 9, 13, 16, and others]. The data on the chemical composition of some rock types were partly published in [10, 11]; in the current work, we consider the composition of all of the studied rock varieties.

MATERIALS AND METHODS

Rock samples were collected from outcrops along the Baikal–Amur Mainline railway (Soloni River) and excavations and quarries along highways on the left bank of the Soloni River and right bank of the El'gandzhya, Chegdomyn, and Umal'ta rivers.

The samples were subjected to mineralogical–petrographic examination under a polarizing microscope (petrographer M.K. Zheverzheeva). The contents of rock-forming oxides were determined in 85 samples by the X-ray fluorescence method in the X-ray spectral analysis laboratory of the Northeast Complex Research Institute, Far East Branch, Russian Academy of Sciences, Magadan (analysts T.D. Borkhodoeva and V.I. Manuilova). The obtained data were processed according to the lithochemistry technique using the Russian algorithm known as the "YuK Standard" [19]. Earlier chemical classifications were also used [12, 24].

BRIEF GEOLOGICAL REVIEW

The Bureya basin (Bb) is considered as being a marginal (foreland) trough [6] on the eastern margin of the Bureya massif, which represents an element of the Jiamusi–Khanka–Bureya superterrane (Fig. 1). In the Jurassic, the Bureya basin was united with other troughs in Russia (Gudzhik, Bira) and China. In the central part of the basin, the Jurassic stratigraphic succession consists of the Lower Jurassic Desh ($J_1dš$), Middle Jurassic Sinkal'ta (J_2sn), Epikan (J_2ep), El'ga (J_2el), Chaganyi ($J_2cğ$), Talyndzhan ($J_{2-3}tl$), and Upper Jurassic Dublikan (J_3db) formations (Fig. 2).

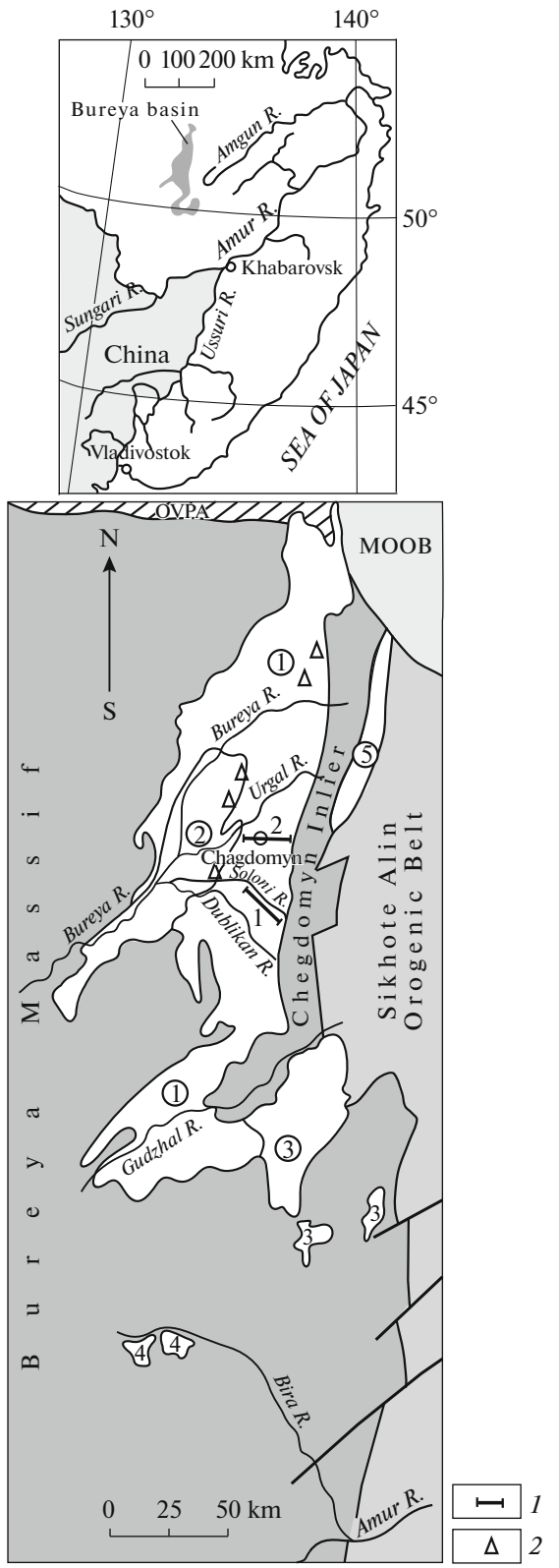

Fig. 1. The Bureya basin and its elements, after [11] with reference to [7]. Troughs (encircled numbers): (1) Bureya, (2) Kyndal, (3) Gudzhik, (4) Bira, (5) Sivak. (MOOB) Mongol–Okhotsk orogenic belt; (OVPA) Ogodzha volcano-plutonic area. Sampling sites: (*1*) sections along the Soloni (1), Chegdomyn and El'gandzhya (2) rivers; (*2*) excavation along highways.

The Cretaceous section includes the Soloni (K_1sn), Cagdamyn ($K_1čg$), Chemchuko ($K_1čm$), Iorek (K_1jr), and Kyndal ($K_{1-2}kn$) formations. The thicknesses of the Jurassic and Cretaceous deposits vary from 4300 to 7500 m and from 2500 to 3500 m, respectively.

The Jurassic–Cretaceous sedimentary succession is represented by alternating conglomerates, gravelly conglomerates, sandstones, siltstones, mudstones, their calcareous and tuffaceous varieties, and acid tuffs (Fig. 2, Photo 1). The sequence exhibits cyclic patterns of different orders reflected in the regular transition from coarse- to fine-grained varieties (from conglomerates to mudstones) [7].

The section along the Soloni River is dominated by siltstones and sandy siltstones accompanied by subordinate mudstones and sandstones. To the southwest and northeast, the share of sandstones increases [1, 7]. The upper part of the section (Upper Jurassic–Lower Cretaceous) includes intercalations and lenses of carbonaceous rocks, coals, and bentonite clays. Significant hiatuses are observed in the upper Toarcian–Aalenian, upper Bajocian, and upper Oxfordian–Kimmeridgian intervals [1, 7].

MINERALOGICAL–PETROGRAPHIC PROPERTIES OF ROCKS

The samples were divided into two selections: sandstones (with prevalence of fine-grained varieties) and clayey–silty rocks (with prevalence of siltstones and sandy siltstones and, less commonly, mudstones).

Sandstones. The rock is grayish–yellowish white, light gray to dark gray (Photo 2). The structure is massive, with thin parallel bedding, mottled, poorly sorted. The contacts between the laminae are even, slightly undulating, discrete, denticulate, distinct, and/or vague. Locally, light sandstone contains filmy laminae of dark material (clayey films or plant detritus). The calcareous varieties are frequently indistinguishable visually from their noncalcareous counterparts. Clasts sized mainly from 0.1 to 0.5 mm across (less commonly 0.05 or 1.0 mm) are angular in shape (Photo 3a–3d). The content of clastic material (quartz, K feldspars, acid plagioclases, micas, various rocks, and accessory minerals) varies from 60–70 to 90–95% and that of cement, from 5–10 to 30–40%.

Accessory minerals (single grains) include zircon, titanite, garnet, zoisite, apatite, tourmaline, hornblende, amphibole, pyroxene, monazite, and ore minerals (from 1–2 to 5%). Authigenic minerals are represented by single grains of glauconite and chlorite (the latter constitutes locally up 1%).

The cement is of the basal, interstitial, filmy, and contact types, being quartz, hydromica, sericite–hydromica, sericite–quartz, calcite, ferruginous, and, rarely, chlorite in composition. In the same thin section, rocks may be characterized by cement of different types. In calcareous sandstones, the cement is

System	Series	Stage	Index	Lithology	Thickness, m	Formation	Sample number
Cretaceous	Upper	Cenomanian	$K_{1-2}kh$		750–1050	Kyndal	–
		Albian					
	Lower	Aptian	K_1ir		550–700	Iorek	–
		Barremian	$K_1čm$		500–600	Chemchuko	<6637
		Hauterivian	$K_1čg$		110–160	Chagdamyn	<6638
		Valanginian	K_1sn		300–400	Soloni	<018-1, 018-2, 018-3
		Berriasian					
Jurassic	Upper	Kimmeridgian	J_3db		220–300	Dublikan	<025-1, 025-2, *6635*, 6635-2, 6636, *6636-1*, *6636-3*
		Oxfordian	$J_{2-3}tl$		330–640	Talyndzhan	<024-1, 024-3 *<014-1, 014-2, 014-3, 015-3, 015-4, 015-5*
		Callovian					
	Middle	Bathonian	$J_2čg$		570–800	Chaganyi	<013-1, 013-3, 013-5, *6632*, *6632-1*, *6632-2* <022-1, 022-2
			J_2el		1370–2530	El'ga	<6624-2 <008-1, 008-3, 008-5, 009-6, 6627 <010-2, 010-3 <011-3, 011-4, 011-8 <012-2, 012-5, 012-7, 6630-1 <021-2, 021-4 <020-1, 020-4 <6640 *<019, 019-2, 019-3* *<6619, 6619-1*
		Bajocian	J_2ep		1660–1800	Epikan	*<007-5, 007-7, 007-8, 6618* *<006-2, 006-3,* 006-4 <005-1, 005-3 <6614-1 <6612-2 *<004-3*
		Aalenian	J_2sn		750–1230	Sinkal'ta	*<6610-4* <6609-2 <003-3, 003-5, 003-6, 003-7 <002-1, *002-2*, 002-7, 002-9 <6642 *<001-1*, *001-2*, *001-3*, 001-4, *6603*
	Lower	Toarcian	$J_1dš$		280–730	Desh	<6602 <6601
		Pliensbachian					

1 *2* *3* *4* *5* *6* *7*

Fig. 2. Schematic stratigraphic section of Jurassic–Lower Cretaceous deposits in the central part of the Bureya sedimentary basin, after [1] modified. (*1*) conglomerates; (*2*) sandstones; (*3*) siltstones; (*4*) mudstones; (*5*) tuffstones; (*6*) tuffaceous siltstones; (*7*) acid tuffs. Sample numbers are given in the Roman type; italics designate clayey–silty rocks. The stratigraphic column corresponds to the sampled interval of the sedimentary sequence.

mostly carbonate. In the triangular classification diagram by Shutov [18], the data points of the sandstones are located in the field of feldspar graywackes (clasts constitute 25–74%), graywacke arkoses, and arkoses (content of rock clasts 8–25%) (Fig. 3). According to the classification by Shvanov [15, 17], in the composition of the magmatic rock clasts in the graywackes, they are divisible into basic, intermediate, and acid varieties. The clasts in the graywackes are dominated by granites and acid (less commonly, basic and intermediate) volcanics, which allows these rocks to be attributed to petroclastic acid graywackes.

Clayey–silty rocks. They are dark gray to black, locally with brownish or slightly whitish tints (calcare-

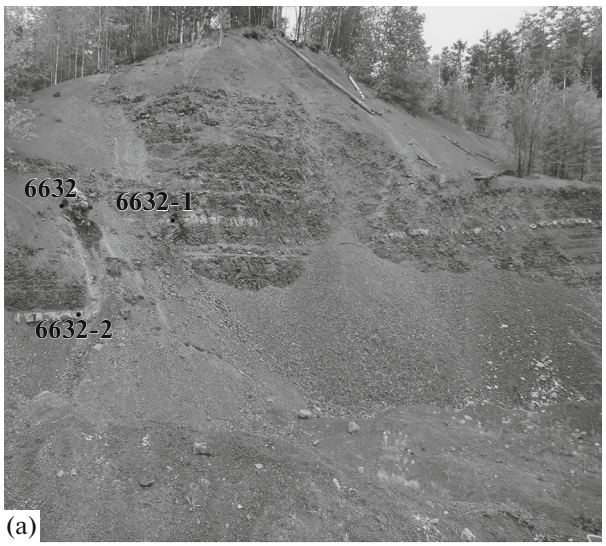

(a)


(b)


(c)

Photo 1. Outcrops of sedimentary rocks on the left side of the Soloni River. (a) light sandstone intercalations (left lower part of the outcrop, observation point 6632-2) and calcareous mudstones (right upper part of the outcrop, observation point 6632-1) among dark clayey–silty rocks of the Chaganyi Formation (observation point 6632), $J_2čg$; (b) massive sandstone of the Epikan Formation, J_2ep; (c) contact between massive sandstones (below) and siltstones with the shelly joint of the Sinkal'ta Formation, J_2sn. All photos were taken by the author except Photo 1a (O.S. Dzyuba).

ous varieties), uniform, slightly mottled or horizontally bedded rocks (Photo 2d). Some samples demonstrate thin inclusions and lenses of black plant detritus. The bedding surfaces are frequently covered by mica accumulations. In the transmitted light, the clayey–silty rocks are gray and their calcareous varieties are brown. The textures are psammitic–aleuritic, aleuritic, and pelitic (Photos 3e–3g). The clasts are usually 0.01–0.10 mm to, less commonly, 0.3 mm in size. Among the clasts, quartz prevails over feldspars and rock fragments.

Tuffs are light pinkish gray, massive and vaguely bedded rocks with rare feldspar crystals. The microtexture is finely aleuritic, ashy, vitrocrystalloclastic (Photo 3h). The content of mineral fragments (dominant quartz, subordinate plagioclase and sericite) may be as high as 40%. They are mainly (60–90%) represented by slightly crystallized acid volcanic ash.

WHOLE-ROCK CHEMICAL COMPOSITION AND CASSIFICATIONS

Oxides in noncarbonate sandstones examined in 48 samples are present in the following quantities (hereinafter, wt %): SiO_2, 62.4–78.2; TiO_2, 0.17–0.88; Al_2O_3, 11.0–15.8; Fe_2O_3, 1.0–7.0; MgO, 0.08–3.37; CaO, 0.1–3.7; Na_2O, 1.32–4.90; K_2O 1.45–5.00 (Fig. 4).[1]

As compared with the sandstones, the clayey–silty rocks (20 samples) are characterized by lower SiO_2 and Na_2O and higher Al_2O_3, Fe_2O_3, and MgO contents: SiO_2, 57.9–67.5; TiO_2, 0.50–0.78; Al_2O_3, 13.5–18.4; Fe_2O_3, 1.9–6.1; MgO, 0.34–4.10; CaO, 0.22–4.20; Na_2O, 0.44–3.30; K_2O 1.47–3.90. In the calcareous varieties, the CaO concentrations exceed 4% (7 and 8 samples of sandstones and clayey–silty rocks, respectively). The tuffs are characterized by relatively high SiO_2 content (comparable with that in the sandstones) and low concentrations of Fe and Mg oxides.

According to the Pettijohn classification [12], most of the sandstones are attributed to graywackes and a minority to arkoses. According to the Herron chemical classification, the clayey–silty varieties belong to shales [24].

Using the techniques recommended by the "YuK Standard" algorithm in [19], the plurality of analytical data was subdivided into 16 clusters and 19 individual analyses, which were excluded from averaging. The so-called "YuK Sialite Standard" was proposed in [19] for description of the lithochemical features of silicate rocks. It uses normalized contents of rock-forming oxides or modules: hydrolysate HM = $(TiO_2 + Al_2O_3 + Fe_2O_3 + FeO + MnO)/SiO_2$, aluminosilicate ASM = Al_2O_3/SiO_2, femic FM = $(Fe_2O_3 + FeO +$

[1] The results of laboratory measurements are completely given in (http://www.itig.as.khb.ru/POG/index.htm)

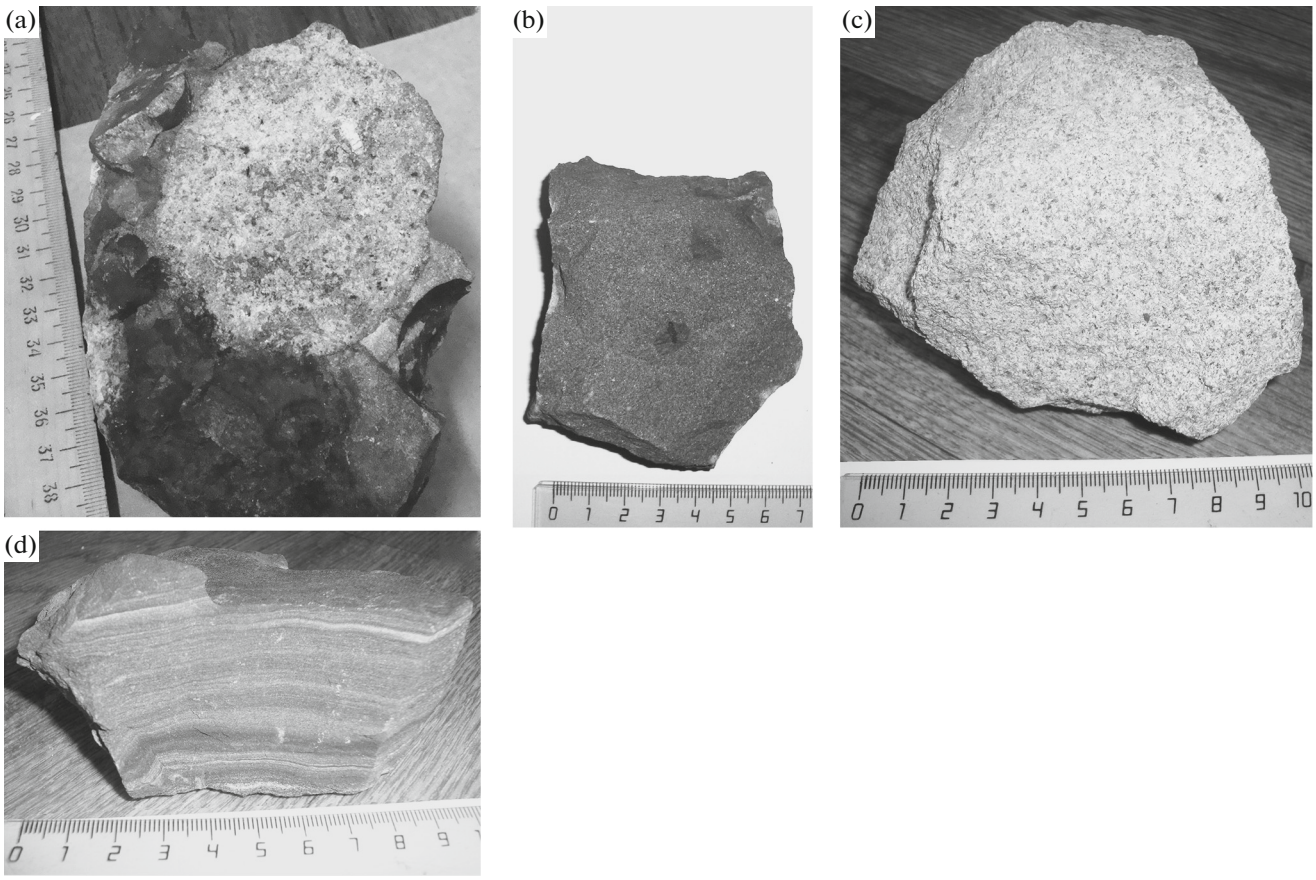

Photo 2. Rock samples. (a) conglomerate of the Desh Formation, $J_1dš$; (b) inequigranular sandstone of the Dublikan Formation, J_3db; (c) fine-grained sandstone of the El'ga Formation, J_2el; (d) laminated siltstone of the Dublikan Formation, J_3db.

MnO + MgO)/SiO_2, titanium TM = TiO_2/Al_2O_3, alkaline AM = Na_2O/K_2O, normalized alkalinity NAM = (Na_2O + K_2O)/Al_2O_3, iron IM (Fe_2O_3 + FeO + MnO)/(TiO_2 + Al_2O_3), sodium SM = Na_2O/Al_2O_3, potassium PM = K_2O/Al_2O_3 (Tables 1, 2).

It should be noted that the normalized alkalinity module (NAM) represents in fact an agpaicity coefficient, which has long been used in petrochemistry [19].

The hydrolysate classification module is the main one. According to the latter, the examined sandstones are attributed to silites (HM < 0.3) and the clayey–silty rocks to sialites (HM = 0.31–0.39), with almost all of them belonging to the subtype of true sialites (MgO contents <3%). During this study, the (Na_2O + K_2O)–HM diagram served as the main one for the clusterization procedure (Fig. 5). This procedure consisted in uniting the spatially closest data points of rocks in the diagram. In the rocks united into compositional clusters, all of the other characteristics were similar. The cluster usually included rocks from a particular formation. The formation could be characterized by one or two clusters and/or several individual compositions.

The feldspars in the *Lower Jurassic graywackes* from the Desh Formation (Table 3, cluster 1) are clas-

Table 1. "Sialite standard:" classes of sialites and siferlites

Class	HM	TM	IM*	FM	NAM	ASM	AM
Hypo-	0.30–0.33	⩽0.030	⩽0.30	⩽0.10	⩽0.20	<0.20	<0.30
Normo-	0.34–0.48	0.030–0.070	0.30–0.55	0.11–0.20	0.21–0.40	0.20–0.35	0.30–1.50
Super-	0.49–0.55	0.071–0.100	0.56–0.70	0.21–0.25	0.41–0.45	0.36–0.40	1.51–3.00
Hyper-	No	>0.100	0.71–0.75	>0.25	>0.45	>0.40	>3.00

* Only for sialites.

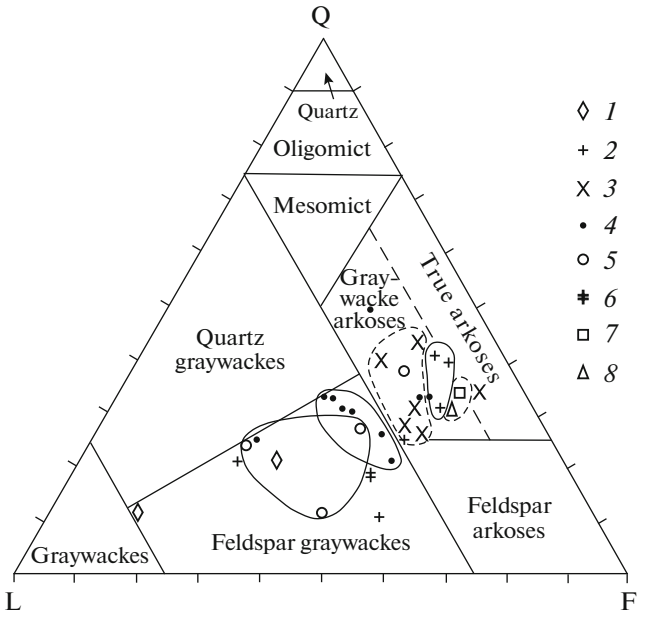

Fig. 3. Rock-forming components of Mesozoic sandstones from the central part of the Bureya basin. Data point of sandstone and fields of formations: (*1*) Desh, (*2*) Sinkal'ta, (*3*) Epikan, (*4*) El'ga, (*5*) Chaganyi, (*6*) Talyndzhan, (*7*) Dublikan, (*8*) Soloni. (Q) quartz, (L) rocks, (F) feldspars.

sified with alkaline supersodium normosilites ($Na_2O + K_2O$ = 5.96%, NAM = 0.47, AM = 1.7, HM = 0.19).

The data points of the *Middle Jurassic sandstones* in the ($Na_2O + K_2O$)–HM diagram form a compact group in the miosilite field, although several of them fall into the normosilite field (Fig. 5). Proceeding from their belonging to a particular formation, several clusters were defined: II and IIa (Sinkal'ta Formation), III and IIIa (Epikan Formation), IV and IVa (El'ga Formation), and V and Va (Chaganyi Formation).

Two data points of arkoses and one data point of graywackes from the lower part of the Sinkal'ta Formation are united into cluster IIa, which is similar in module values to cluster I ($Na_2O + K_2O$ = 5.7%, NAM = 0.50, AM = 2.88, HM = 0.18). Clusters I and IIa are lithochemically identical to each other, being characterized by different petrographic compositions. The rock fragments in the graywackes constitute 47–74% (calculated for 100%) and they are represented by granites, pegmatites, acid (less commonly, intermediate) volcanics, and rare sedimentary rocks. The quartz content is as high as 13–21%. The arkoses are characterized by higher quartz content (25–41%) and lower share of rock fragments (12–15%). The acid igneous rocks enriched with silica oxide determine its high concentration in the graywackes of the Desh Formation. Therefore, it is unreasonable to unite clusters I and IIa, although this seems logical from the point of view of lithochemistry.

The high NAM and AM values indicate the presence of feldspars and good preservation of plagioclases, while the low TM, FM, and IM values (TM = 0.015 and 0.018, FM = 0.03–0.04, I = 0.14–0.20) characteristic of rocks from clusters I and IIa, respectively, imply the acid composition of the parent rocks, represented by acid volcanics and subordinate granites and sedimentary rocks.

The sandstones of Middle Jurassic clusters II–V are generally classified as alkaline miosilites ($Na_2O + K_2O$ = 5.35–7.21; HM = 0.22–0.30), normal with respect to all other parameters except AM, according to which they are classified with supersodium rocks (AM = 0.83–2.36). It should be noted in addition that some compositions of these rocks are characterized by high values of normalized alkalinity module (NAM = 0.52–0.57), according to which they are attributed to superalkaline rocks.

The difference between clusters IIa and II consists in lower values of almost all modules. The exceptions are NAM (0.50 and 0.46, respectively) and especially AM (2.88 and 0.83, respectively). The difference in the NAM values indicates that the sandstones from cluster IIa are characterized by higher quartz and lower feldspar concentrations. At the same time, the individual composition of the greywacke (sample 6609-2, Sinkal'ta Formation) with the higher NAM value (0.53) demonstrates the moderate content of quartz (21%) and simultaneously the abundance of rock fragments (53%).

The calcareous sandstones forming clusters IIIa (Epikan Formation) and Va (Chaganyi Formation) are expectedly attributed to miosilites. In their values

Table 2. Classes of silites

Class	HM	TM	IM*	FM	NAM	ASM	AM
Hypo-	0.20–0.30	⩽0.020	⩽0.20	⩽0.03	⩽0.20	⩽0.05	⩽0.20
Normo-	0.11–0.20	0.021–0.080	0.21–0.70	0.04–0.10	0.21–0.50	0.06–0.20	0.21–0.80
Super-	0.051–0.10	0.081–0.120	0.71–1.0	0.11–0.15	0.51–0.70	>0.20	0.81–2.50
Hyper-	⩽0.05	>0.120	>1.0	>0.15	>0.70	No	>2.50

(HM) hydrolysate module ($TiO_2 + Al_2O_3 + Fe_2O_3 + FeO + MnO)/SiO_2$; (TM) titanium module TiO_2/Al_2O_3; (IM) iron module ($Fe_2O_3 + FeO + MnO)/(TiO_2 + Al_2O_3$); (FM) femic module ($Fe_2O_3 + FeO + MnO + MgO)/SiO_2$; (NAM) normalized alkalinity module ($Na_2O + K_2O/Al_2O_3$); (ASM) aluminosilicate module Al_2O_3/SiO_2; (AM) alkaline module Na_2O/K_2O.

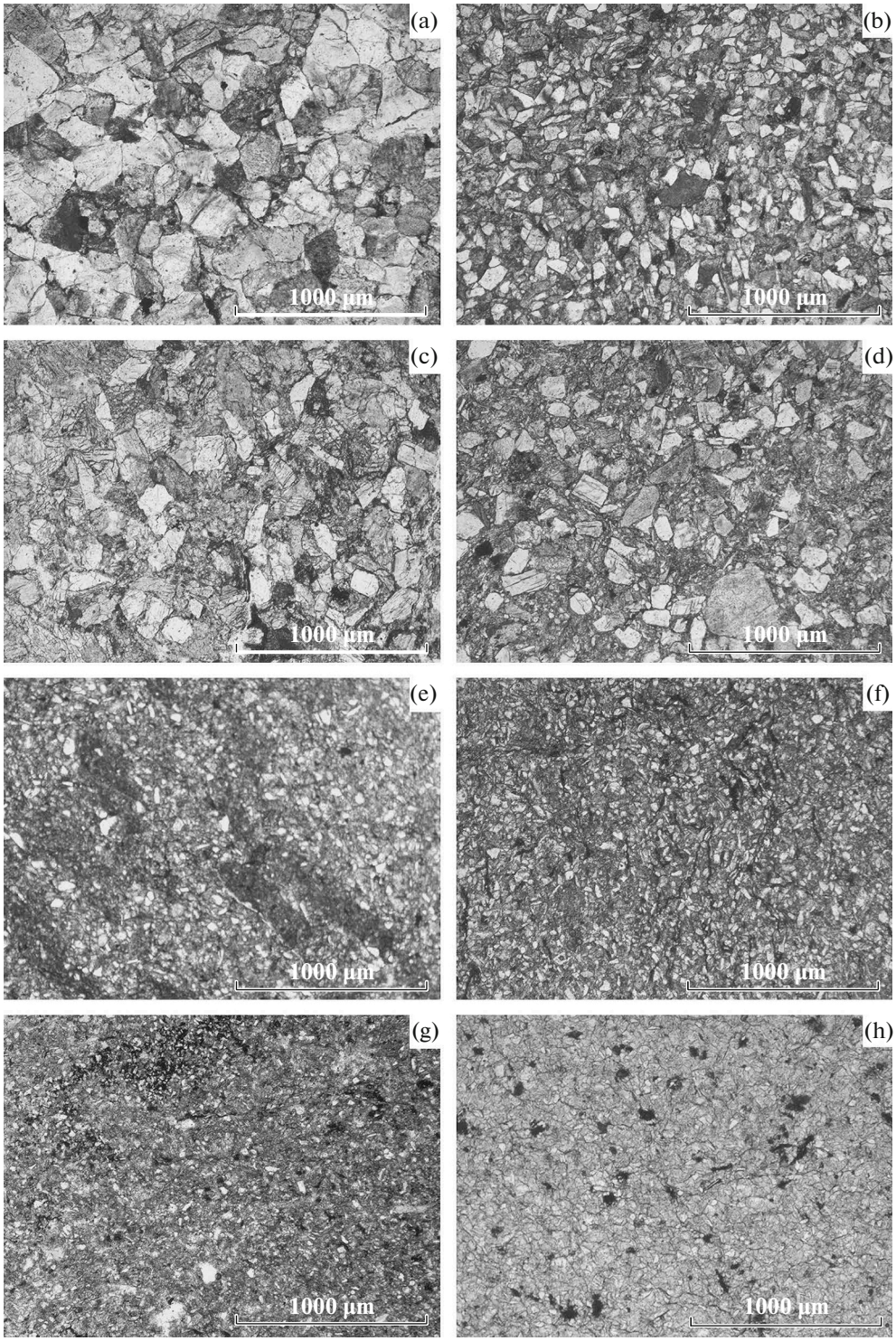

Photo 3. Thin sections of main rock types from the Bureya basin. Sandstones: (a) greywacke arkose of the Sinkal'ta Formation, J_2sn, Soloni River; (b) greywacke arkose of the Epikan Formation, J_2ep, Soloni River; (c) feldspar greywacke of the Chaganyi Formation, $J_2čg$, El'gandzhya River; (d) quartz feldspar greywacke of the El'ga Formation, J_2el, Soloni River. Siltstones: (e) Epikan Formation J_2ep, Soloni River; (f) El'ga Formation, J_2el, El'gandzhya River; (g) calcareous siltstone of the Talyndzhan Formation, J_2tl, Soloni River; (h) acid ashy tuff of the El'ga Formation, J_2el, Soloni River. Parallel nicols.

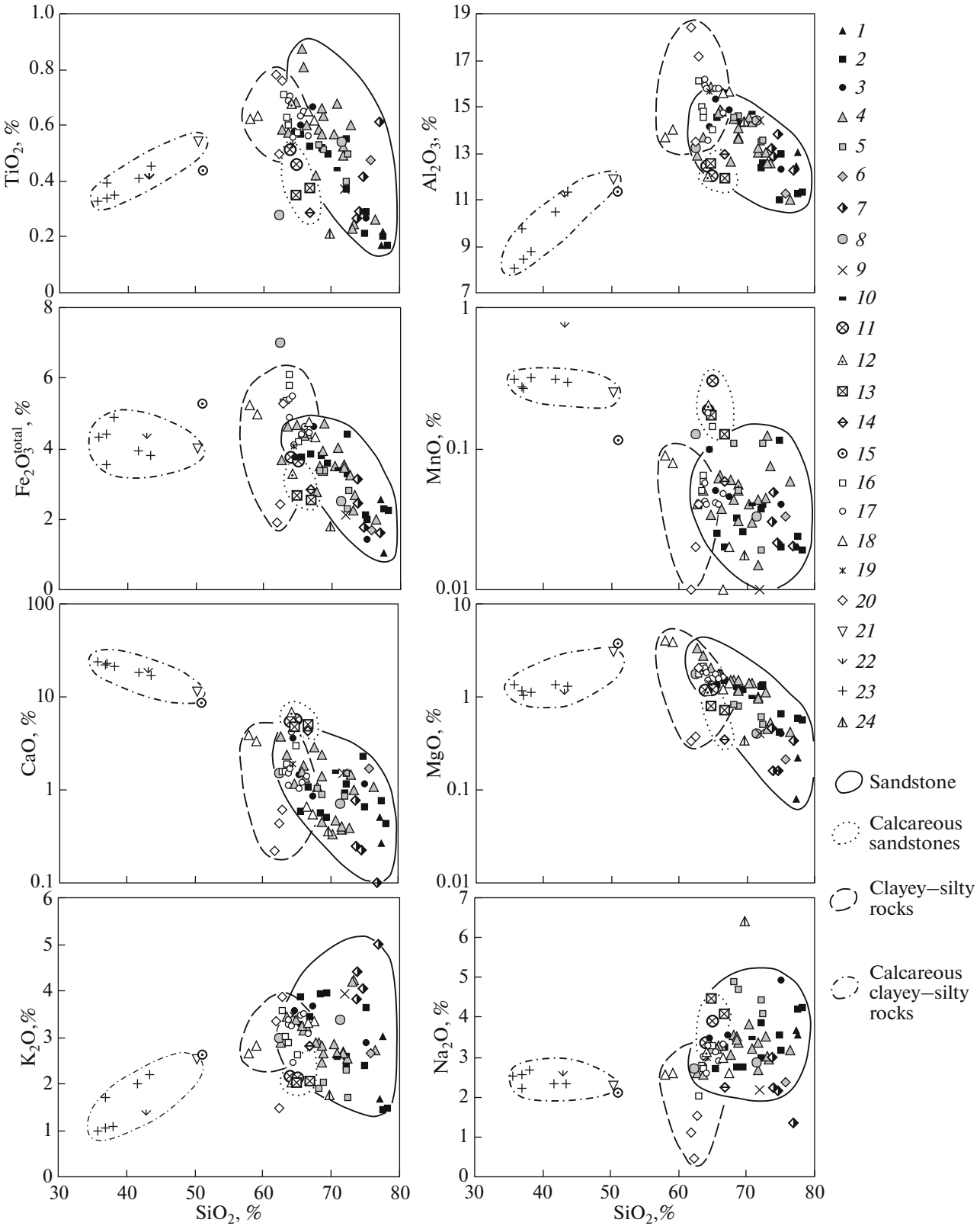

Fig. 4. Variation diagrams for Jurassic–Lower Cretaceous rocks of the Bureya basin. (*1–10*) sandstones of formations: (*1*) Desh, (*2*) Sinkal'ta, (*3*) Epikan, (*4*) El'ga, (*5*) Chaganyi, (*6*) Talyndzhan, (*7*) Dublikan, (*8*) Soloni, (*9*) Chagdamyn, (*10*) Chemchuko; (*11–15*) calcareous sandstones of formations: (*11*) Epikan, (*12*) El'ga, (*13*) Chaganyi, (*14*) Talyndzhan, (*15*) Soloni; (*16–20*) clayey–silty rocks of formations: (*16*) Sinkal'ta, (*17*) Epikan, (*18*) El'ga, (*19*) Chaganyi, (*20*) Dublikan; (*21–23*) calcareous clayey–silty rocks of formations: (*21*) El'ga, (*22*) Chaganyi, (*23*) Talyndzhan; (*24*) tuff of the El'ga Formation.

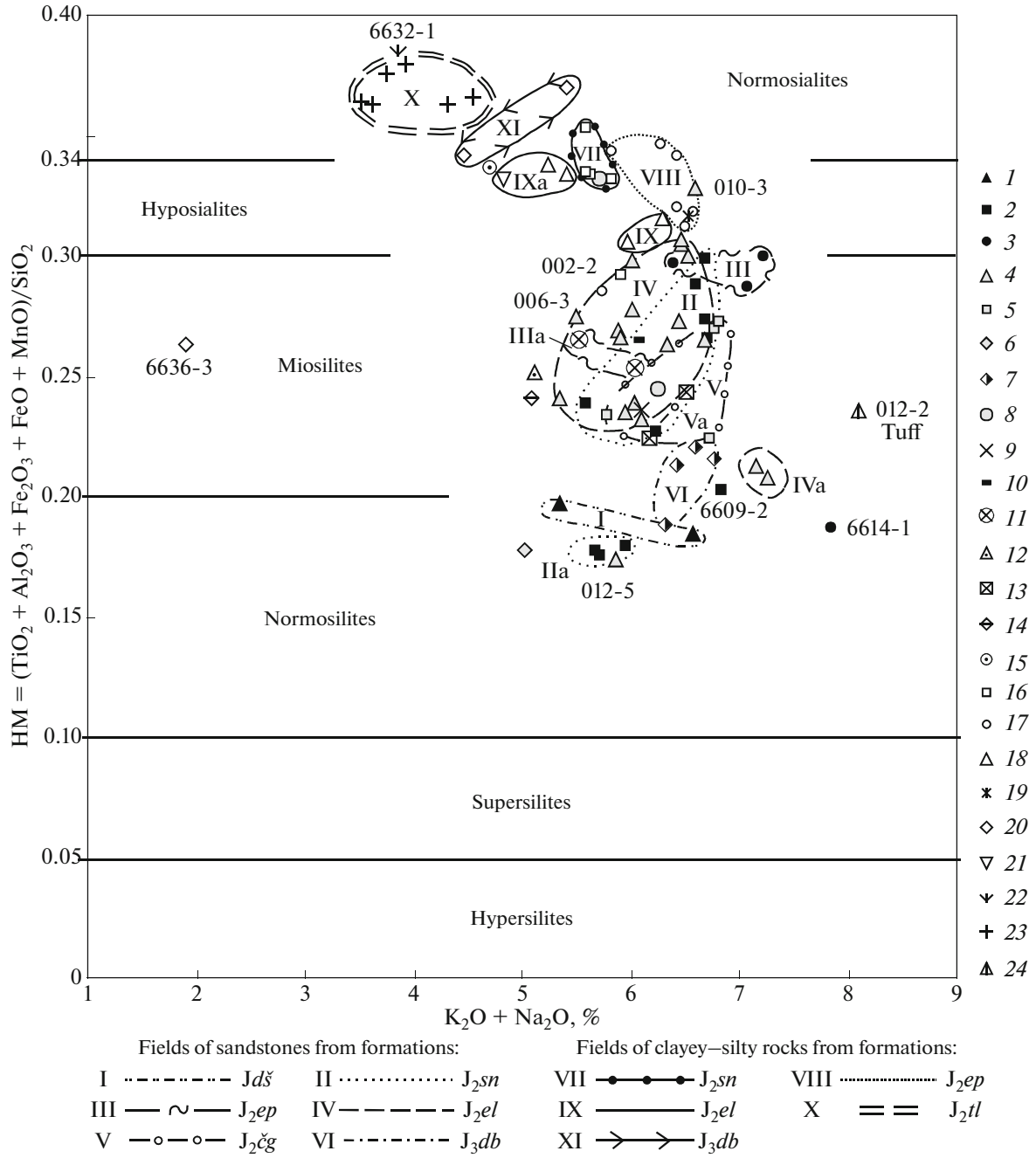

Fig. 5. The (K_2O+Na_2O)–HM diagram for Jurassic–Lower Cretaceous rocks of the Bureya basin. (*1–10*) sandstones of formations: (*1*) Desh, (*2*) Sinkal'ta, (*3*) Epikan, (*4*) El'ga, (*5*) Chaganyi, (*6*) Talyndzhan, (*7*) Dublikan, (*8*) Soloni, (*9*) Chagdamyn, (*10*) Chemchuko; (*11–15*) calcareous sandstones of formations: (*11*) Epikan, (*12*) El'ga, (*13*) Chaganyi, (*14*) Talyndzhan, (*15*) Soloni; (*16–20*) clayey–silty rocks of formations: (*16*) Sinkal'ta, (*17*) Epikan, (*18*) El'ga, (*19*) Chaganyi, (*20*) Dublikan; (*21–23*) calcareous clayey–silty rocks of formations: (*21*) El'ga, (*22*) Chaganyi, (*23*) Talyndzhan; (*24*) tuff of the El'ga Formation.

of modules, these clusters are similar to clusters III and V, differing mainly in higher CaO contents (Fig 4, Table 3), which is their distinguishing characteristic. They also exhibit elevated MnO concentrations.

The individual composition of the arkose in sample 6614-1 from the Epikan Formation differs from that in clusters III and IIIa in its high SiO_2 (75%), total alkalis (7.83), high NAM (0.64), and lowered iron (IM = 0.12, hypoferrous) and femic (FM = 0.02, hypofemic) values. The rock is classified with superalkaline normosilite (HM = 0.19). This is most likely explained by the elevated contents of quartz fragments (44% versus 26–34% in the rocks of clusters III and IIIa).

Table 3. Chemical composition of sandstones from the Bureya basin

Formations	Desh	Sinkal'ta			Epikan			
clusters/compositions outside of clusters	I	II	IIa	6609-2	III	IIIa	6614-1	
chemotypes	normosilite	miosilite	normosilite	miosilite	miosilite	carbonate-bearing miosilite	normosilite	
number of samples	2	6	3	1	3	2	1	
SiO_2	77.38	68.93	77.46	75.10	66.58	64.43	75.02	
TiO_2	0.20	0.52	0.20	0.29	0.58	0.49	0.27	
Al_2O_3	12.75	14.36	11.24	12.97	14.75	12.26	12.32	
Fe_2O_3	1.79	3.79	2.24	1.97	4.44	3.70	1.41	
MnO	0.02	0.03	0.02	0.02	0.05	0.25	0.04	
MgO	0.15	1.32	0.57	0.66	1.36	1.23	0.40	
CaO	0.39	0.76	0.76	0.67	1.43	5.57	1.15	
Na_2O	3.62	2.88	4.21	3.18	3.48	3.62	4.94	
K_2O	2.34	3.65	1.47	3.64	3.58	2.16	2.89	
P_2O_5	0.06	0.11	0.07	0.06	0.15	0.13	0.06	
L.O.I.	1.32	3.62	1.63	1.44	3.94	6.10	1.50	
Sum	100.00	99.90	99.93	100.00	99.91	99.92	100.00	
$Na_2O + K_2O$	5.96	6.63	5.70	6.82	7.06	5.77	7.83	
HM	0.19	0.27	0.18	0.20	0.30	0.26	0.19	
IM	0.14	0.25	0.20	0.15	0.29	0.31	0.12	
FM	0.03	0.08	0.04	0.04	0.09	0.08	0.02	
ASM	0.16	0.21	0.15	0.17	0.22	0.19	0.16	
TM	0.015	0.035	0.018	0.022	0.041	0.040	0.022	
NAM	0.47	0.46	0.50	0.53	0.48	0.47	0.64	
AM	1.70	0.83	2.88	0.87	0.97	1.68	1.71	
SM	0.28	0.20	0.37	0.25	0.24	0.30	0.40	
PM	0.18	0.24	0.13	0.28	0.25	0.18	0.23	
Formations	El'ga					Chaganyi		
clusters/compositions outside of clusters	IV	IVa	010-3	012-5	6624-2	V	Va	
chemotypes	miosilite		hyposialite	normosilite	carbonate-bearing miosilite	miosilite	carbonate-bearing miosilite	
number of samples	15	2	1	1	1	4	2	
SiO_2	68.64	73.17	64.76	76.33	64.17	70.50	65.80	
TiO_2	0.59	0.24	0.69	0.26	0.67	0.51	0.36	
Al_2O_3	13.71	12.60	15.84	10.97	11.95	14.06	12.23	
Fe_2O_3	3.66	2.45	4.67	2.00	3.23	3.08	2.63	
MnO	0.04	0.10	0.03	0.06	0.20	0.08	0.15	
MgO	1.49	0.49	2.07	0.42	1.11	0.72	0.75	
CaO	1.34	1.23	1.15	1.06	6.72	0.98	4.97	
Na_2O	3.30	2.99	3.22	3.16	3.11	4.58	4.30	
K_2O	2.85	4.22	3.37	2.71	2.00	1.97	2.04	
P_2O_5	0.14	0.05	0.17	0.06	0.15	0.15	0.12	
L.O.I.	3.87	2.40	3.95	2.87	6.69	3.58	6.59	
Sum	99.92	99.91	99.92	99.90	100.00	99.92	99.93	

Table 3. (Contd.)

$Na_2O + K_2O$	6.03	7.21	6.59	5.87	5.11	6.75	6.34	
HM	0.27	0.21	0.33	0.17	0.25	0.25	0.23	
IM	0.27	0.20	0.28	0.18	0.27	0.22	0.22	
FM	0.08	0.04	0.10	0.03	0.07	0.05	0.05	
ASM	0.20	0.17	0.24	0.14	0.19	0.20	0.19	
TM	0.042	0.019	0.043	0.024	0.056	0.036	0.030	
NAM	0.44	0.57	0.42	0.54	0.43	0.47	0.52	
AM	1.21	0.71	0.96	1.17	1.56	2.36	2.11	
SM	0.24	0.24	0.20	0.29	0.26	0.33	0.35	
PM	0.20	0.34	0.21	0.25	0.17	0.13	0.17	
Formations	Talyndzhan		Dublikan	Soloni			Chagdamyn	Chemchuko
clusters/compositions outside of clusters	024-1	024-3	VI	018-2	018-3	018-1	6638	6637
chemotypes	normosilite	carbonate-bearing miosilite	miosilite	miosilite	hyposialite	carbonate-bearing pseudohyposialite	miosilite	miosilite
number of samples	1	1	4	1	1	1	1	1
SiO_2	75.79	66.77	74.26	71.37	62.39	51.04	71.87	70.36
TiO_2	0.47	0.29	0.35	0.539	0.28	0.44	0.37	0.44
Al_2O_3	11.26	12.97	13.00	14.43	13.26	11.36	14.42	14.74
Fe_2O_3	1.70	2.84	2.08	2.49	7.02	5.27	2.14	3.43
MnO	0.03	0.06	0.03	0.033	0.128	0.12	0.01	0.04
MgO	0.21	0.35	0.25	0.4	1.79	3.71	0.41	1.00
CaO	1.72	4.31	0.24	0.71	1.49	8.44	1.52	1.58
Na_2O	2.38	2.26	2.18	2.85	2.73	2.09	2.17	3.48
K_2O	2.65	2.83	4.21	3.39	2.99	2.61	3.92	2.56
P_2O_5	0.07	0.06	0.04	0.14	0.074	0.13	0.07	0.10
L.O.I.	3.62	7.19	2.58	3.55	7.77	14.72	3.10	2.28
Sum	99.91	99.92	99.96	99.90	99.92	99.93	100.00	100.01
$Na_2O + K_2O$	5.03	5.09	6.46	6.24	5.72	4.70	6.09	6.04
HM	0.18	0.24	0.21	0.25	0.33	0.34	0.24	0.27
IM	0.15	0.22	0.15	0.17	0.53	0.46	0.15	0.23
FM	0.03	0.05	0.03	0.04	0.14	0.18	0.04	0.06
ASM	0.15	0.19	0.18	0.20	0.21	0.22	0.20	0.21
TM	0.042	0.022	0.03	0.037	0.021	0.038	0.026	0.030
NAM	0.45	0.39	0.51	0.43	0.43	0.41	0.42	0.41
AM	0.90	0.80	0.52	0.84	0.91	0.80	0.55	1.36
SM	0.21	0.17	0.16	0.20	0.21	0.18	0.15	0.24
PM	0.24	0.22	0.32	0.23	0.23	0.23	0.27	0.17

The El'ga graywackes in the El'gandzha River section (cluster IVa) are attributed to superalkaline miosilites (NAM = 0.57; HM = 0.21).

They differ from the sandstones of cluster IV in the higher prevalence of K_2O over Na_2O, higher SiO_2 and total alkali contents, and, correspondingly, lower values of all modules except for NAM and AM (Table 3). The detrital material contains abundant quartz (approximately 30%) and rock fragments (30%) are represented by acid volcanics, volcanic glasses, quartzites, and fine-grained granites.

The individual composition of the graywacke (sample 012-5, El'ga Formation) differs from clusters IV and IVa in its high SiO_2 contents (76.3%) and NAM value (0.54) against the background of lowered IM and FM values (0.18 and 0.03, respectively). It is identified as hypoferrous and hypofemic superalkaline normosilite (HM = 0.17). Such properties of this rock

are primarily explained by its petrographic composition: quartz, 25%; feldspars, 25% (equal proportions of plagioclase and K feldspars); rock fragments represented largely by acid volcanics, volcanic glasses, rare quartzites, and mudstones, 50% (greywacke). The peculiar composition of another sandstone from the El'ga Formation (sample 010-3), which is classified as superalkaline normosodium hyposialite, is most likely determined by the relatively higher cement content.

The arkoses from the Upper Jurassic Dublikan Formation (cluster VI) are generally identified as superalkaline (NAM = 0.51) normosodium miosilites (HM = 0.21). In these rocks, K_2O prevails considerably over Na_2O (the lowest AM (0.52) among all clusters), which makes the Dublikan sandstones different from most sandstone varieties in other formations.

The position of the data points of the rocks in the (Na_2O+K_2O)–HM diagram, belonging to different formations (compositions of samples 018-2, 6637, 6638) and different classes (compositions of samples 018-1–018-3 from the Soloni Formation) gives reason to characterize every Lower Cretaceous sandstone separately (Table 3).

Two sandstone samples from the Soloni Formation, one of which is calcareous (sample 018-1, CaO = 8.44%, SiO_2 = 51%), are classified as superalkaline (NAM = 0.41–0.43) hyposialites (HM = 0.330–0.337) normal with respect to all other modules. At the same time, the calcareous sandstone (sample 018-1) contains MgO = 3.71% and, thus, should be considered as pseudohyposialite (Table 3).

The sandstones from the Soloni (sample 018-2), Chagdamyn, and Chemchuko formations are attributed to normal miosilites (HM = 0.24–0.27), but the compositions of samples 018-2 and 6637 are supersodium according to the alkaline module.

With respect to IM and FM, the miosilite from the Chagdamyn Formation is hypoferrous, close to hypofemic, which makes it similar to the Talyndzhan normosilite and Dublikan miosilites.

The middle Jurassic *clayey–silty rocks* of the Sinkal'ta, Epikan, El'ga (clusters VII, VIII, IX), and Chaganyi (sample 6632) formations are generally classified as hyposialites (HM = 0.31–0.33), alkaline with respect to total alkalinity (Na_2O + K_2O = 5.6–6.4%) and normal with respect to other modules (Table 4).

The calcareous siltstone (sample 019-1) and two siltstone samples from the El'ga (cluster IXa) with MgO content exceeding 3% are identified on average as carbonate-bearing pseudohyposialite.

Six samples of calcareous clayey–silty rocks from the Talyndzhan Formation are classified as carbonate superalkaline supersodium normosialites (HM = 0.37, CaO = 22%, NAM = 0.42, AM = 1.87).

Three samples of clayey siltstone from the Dublikan Formation (cluster XI) are identified as hypoferrous, hypofemic normosialites (HM = 0.35, IM = 0.20, FM = 0.08), normal with regard to other modules.

Based on total alkalis, the sandstones (clusters I–VI) and clayey–silty rocks of pre-Late Jurassic age (hyposialites of clusters VII–IX) are considered as being alkaline (Na_2O + K_2O = 5.00–7.25%), while the Upper Jurassic clayey–silty rocks (normosialites of clusters X, XI) demonstrate no elevated total alkalinity (Na_2O + K_2O = 3.84 and 4.94, respectively).

No specific values of the modules are recorded in individual carbonate-bearing rocks and their clusters. Carbonate in the sandstones is present in rock cement and, locally, in the form of faunal remains.

The calcareous mudstone of the Chaganyi Formation (sample 6632-1) taken from an intercalation approximately 30–40 cm thick occurring among normal clayey–silty varieties (Photo 1a) is classified as carbonate (CaO = 18.2%) normoalkaline (Na_2O + K_2O = 3.85%) supersodium (AM = 1.94) normosialite (HM = 0.39).

The *tuff* from the El'ga Formation (sample 012-2) is identified as alkaline miosilite (HM = 0.23). In its total alkalinity of 8.04% (type of alkalites), the rock sharply differs from the other varieties (Fig. 5, Table 4). The difference between the tuff and some sandstones in the SiO_2 and Al_2O_3 contents and HM values is less notable. It appears that some sandstones classified as normosilites are characterized by values of modules similar to their counterparts in tuffs, which hampers their reliable diagnostics. Nevertheless, the low TM values and elevated total alkalinity in the tuffs (like in rhyolites) [19] make it necessary to verify the correctness of the tuff definition by lithochemical methods. In their lower values of all modules and lower content of femic elements, the tuffs are most different from the clayey–silty rocks (Fig. 6).

DISCUSSION

In accordance with the "YuK Standard" [19], the sandstones are classified based on their lithochemical parameters as silites (normo- and mio-) and the clayey–silty rocks, as sialites (normo- and hypo-); i.e., the lithochemical characteristics of the rocks depend on their grain-size composition, which is a usual situation in lithochemsitry.

The generally high values of the aluminosilicate (ASM), sodium (SM), and alkaline (AM) modules and the practically uniform hydrolysate (HM) module, which serves as a quantitative measure of supergene differentiation of material, indicate the immaturity of the Lower–Middle Jurassic sandstones. At the same time, the values of these modules for the Upper Jurassic–Lower Cretaceous rocks of the Dublikan, Soloni, and Chagdamyn formations imply their substantially higher degree of maturity as compared with the underlying deposits.

Table 4. Chemical composition of clayey–silty rocks from the Bureya basin

Formations	Sinkal'ta		Epikan		El'ga		Chaganyi
clusters/compositions outside of clusters	VII	002-2	VIII	006-3	IX	IXa	6632
chemotypes	hyposialite	miosilite	hyposialite	miosilite	hyposialite	carbonate-bearing pseudohypo-sialite	hyposialite
number of samples	4	1	6	1	2	3	1
SiO_2	63.47	64.98	64.74	64.29	67.02	57.94	64.36
TiO_2	0.62	0.58	0.67	0.56	0.64	0.62	0.53
Al_2O_3	14.92	14.03	15.78	13.54	15.61	13.66	15.66
Fe_2O_3	5.59	4.21	4.75	4.10	4.55	4.98	4.05
MnO	0.05	0.15	0.04	0.18	0.02	0.09	0.10
MgO	1.99	1.56	1.80	1.52	1.31	3.87	1.41
CaO	1.69	3.02	1.35	4.18	0.60	3.82	1.89
Na_2O	2.73	3.28	3.01	3.28	2.79	2.57	2.98
K_2O	2.96	2.62	3.33	2.45	3.34	2.66	3.54
P_2O_5	0.18	0.17	0.17	0.17	0.16	0.16	0.11
L.O.I.	5.63	5.32	4.17	5.67	4.00	9.12	5.37
Sum	99.92	99.91	99.92	99.94	100.00	99.918	100.00
$Na_2O + K_2O$	5.61	5.90	6.42	5.73	6.12	5.23	6.52
HM	0.33	0.29	0.33	0.29	0.31	0.33	0.32
IM	0.36	0.30	0.29	0.30	0.28	0.34	0.26
FM	0.12	0.09	0.10	0.09	0.09	0.15	0.09
ASM	0.24	0.22	0.24	0.21	0.23	0.24	0.24
TM	0.042	0.041	0.042	0.041	0.041	0.046	0.034
NAM	0.38	0.42	0.40	0.42	0.39	0.39	0.42
AM	0.93	1.25	0.90	1.34	0.84	0.93	0.84
SM	0.18	0.23	0.19	0.24	0.18	0.19	0.19
PM	0.20	0.19	0.21	0.18	0.21	0.20	0.23
Formations	Chaganyi	Talyndzhan	Dublikan		El'ga	Mesozoic granite, after [3, 14]	
clusters/compositions outside of clusters	6632-1	X	XI	6636-3	012-2 tuff		
chemotypes	carbonate normosialite	carbonate normosialite	normosialite	miosilite	miosilite		
number of samples	1	6	2	1	1	4	
SiO_2	43.02	37.55	62.35	62.34	69.05	70.81	
TiO_2	0.42	0.37	0.77	0.50	0.20	0.38	
Al_2O_3	11.11	9.29	17.80	13.46	14.28	15.80	
Fe_2O_3	4.34	4.12	3.59	2.44	1.72	2.92	
MnO	0.72	0.30	0.03	0.02	0.02	0.04	

Table 4. (Contd.)

MgO	1.02	1.25	1.19	0.38	0.32	0.58	
CaO	18.18	21.89	0.42	0.44	0.34	2.29	
Na_2O	2.54	2.45	1.32	0.44	6.34	3.69	
K_2O	1.31	1.40	3.62	1.47	1.70	3.34	
P_2O_5	0.15	0.27	0.12	0.02	0.04	0.11	
L.O.I.	17.17	21.17	8.81	18.49	5.92		
Sum	99.98	99.97	100.00	100.00	99.93	99.64	
Na_2O+ K_2O	3.85	3.84	4.94	1.91	8.04	7.02	
HM	0.39	0.37	0.36	0.26	0.23	0.27	
IM	0.44	0.46	0.20	0.18	0.12	0.19	
FM	0.14	0.14	0.08	0.05	0.03	0.05	
ASM	0.26	0.24	0.29	0.22	0.21	0.22	
TM	0.038	0.040	0.043	0.037	0.014	0.024	
NAM	0.35	0.42	0.28	0.14	0.56	0.46	
AM	1.94	1.87	0.36	0.30	3.73	1.13	
SM	0.23	0.26	0.07	0.03	0.44	0.24	
PM	0.12	0.15	0.20	0.11	0.12	0.21	

Values of normalized alkalinity (NAM) exceeding 0.4 suggest the presence of feldspars. High values of the alkaline module (AM > 1) indicate well-preserved plagioclases acted as alkali carriers in most Lower–Middle Jurassic rocks. The Late Jurassic Epoch was marked by intensified chemical weathering, which resulted in the destruction of plagioclases and Na removal, evident from the lowered alkaline module (AM < 1) of the overlying sandstones of the Talyndzhan (AM = 0.90), Dublikan (AM = 0.52), Soloni (AM = 0.85), and Chagdamyn (AM = 0.55) formations. Inasmuch as rock maturity represents an indicator of the intensity of chemical weathering, which is a climate-dependent process, the warmest climate during the considered time interval is reconstructed for the Late Jurassic Epoch. This inference follows from the postulate that according to [23, 25, 27], the indices of chemical weathering CIW (CIW = $([Al_2O_3/(Al_2O_3 + CaO + Na_2O)] \times 100$) and CIA ($([Al_2O_3/(Al_2O_3 + CaO^* + Na_2O + K_2O)] \times 100$) in the shales, which amount to approximately 80 and 70, respectively, are considered as marking the lithochemical boundary between the cold and warm climates. For the sandstones, the CIW and CIA values are lower.

The presented data show that the warm climate existed only during the Late Jurassic Epoch (Table 5, Fig. 7); during other periods, the climate was temperate. It should, however, be taken into consideration that the degree of rock alteration is also determined by the relief, which depends on the tectonic setting. In differentiated mountainous systems (intense tectonic activity), physical weathering prevails even in warm climatic environments. At the same time, physical weathering is mostly characteristic of plains (calm tectonic settings) under dry climatic conditions. It is believed that changes to the flora are more informative. Unfortunately, findings of fossil plant remains are recorded only in a small part of the distribution area of terrigenous rocks. In the Bureya basin, the warm humid Late Jurassic–Early Cretaceous climate is confirmed by the presence of many coal seams, the formation of which is related to the abundant and diverse vegetation that existed there at that time. The available reconstructions of climate changes in the Bureya basin obtained by different methods coincide. Prior to the Late Jurassic, the provenances were characterized by differentiated topography and the cold climate stimulated wide development of physical weathering. For the terminal Jurassic–initial Cretaceous, leveled relief and temperate humid climate are reconstructed.

A.A. Migdisov demonstrated that dynamic sorting of detrital material (natural panning) increases the content of Ti minerals in sandstones, which usually results in increase of their titanium module (TM) as compared with clayey–silty rocks. Ya.E. Yudovich named this property as the *Migdisov regularity* [19].

No Migdisov regularity is documented in the Lower–Middle Jurassic rocks: the median TM values in the sandstones are lower, although insignificantly, as compared with this parameter in the clayey–silty rocks (Tables 3, 4). Consequently, disintegrated material was deposited during a relatively short period, which is characteristic of tectonically active structures with highly differentiated mountainous relief. Although the terminal Jurassic–initial Cretaceous was

characterized, according to reconstructions, by relatively calm tectonic activity and relief leveling, the Migdisov regularity in the rocks of this age is also indistinct. This may be explained by low-energy hydrodynamic activity in swamping basins, which accumulated coals, while transported ashy material rapidly covered drifts and prevented panning [5].

These facts allow an assumption that the terrigenous rocks inherited the composition of the parent rocks. The given composition of the examined rocks is also evident from the positive correlation between FM and IM, TM and IM (Fig. 6) and the negative correlation between NAM and HM; i.e., they represent rocks of the first cycle [19].

In the tuff, the high total alkalinity and low HM, TM, FM, and IM values serve as indicators of the acid composition and volcanic origin of this rock. At the same time, the lithochemical parameters alone are insufficient for correct discrimination between acid tuffs and purely terrigenous rocks (superalkaline sandstones). With sufficient experience, the tuffs can be distinguished visually from their structural–textural features and coloration; under a microscope the determination can be made with full confidence.

Genesis of terrigenous rocks and provenances. The detrital rocks represent indicators of the composition of rocks developed in the provenances. Nevertheless, it should be noted that their petrographic composition is identical to that of the parent rocks only at the earliest stages of clastics formation. The composition of the rock fragments and accessory minerals in the sandstones allows granite gneisses and acid magmatites to be considered as their main parent rocks. Sedimentary rocks—sandstones and clayey–silty varieties—make up a small share in the composition of the parent rocks.

Table 5. Variations of chemical weathering indices (CIA and CIW) in rocks of the Bureya sedimentary basin

	Sandstones				Clayey–silty rocks	
	J_1	J_2	J_3	K_1	J_2	J_3
CIA						
min	58	47	53	56	46	69
Average	**58**	**55**	**58**	**57**	**57**	**75**
max	59	62	62	60	64	81
CIW						
min	64	52	62	63	51	83
Average	**66**	**63**	**73**	**67**	**65**	**87**
max	67	72	84	71	75	90
n	2	37	5	4	17	3

(min) minimum value; (max) maximum value, (*n*) number of samples.

In the F1–F2 factor diagram for the chemical composition of the primary rocks [26], the data points of the examined sandstones and clayey–silty rocks are mostly located in the field of acid volcanics. Moreover, the data points of the clayey–silty rocks are drawn toward the field of intermediate volcanics

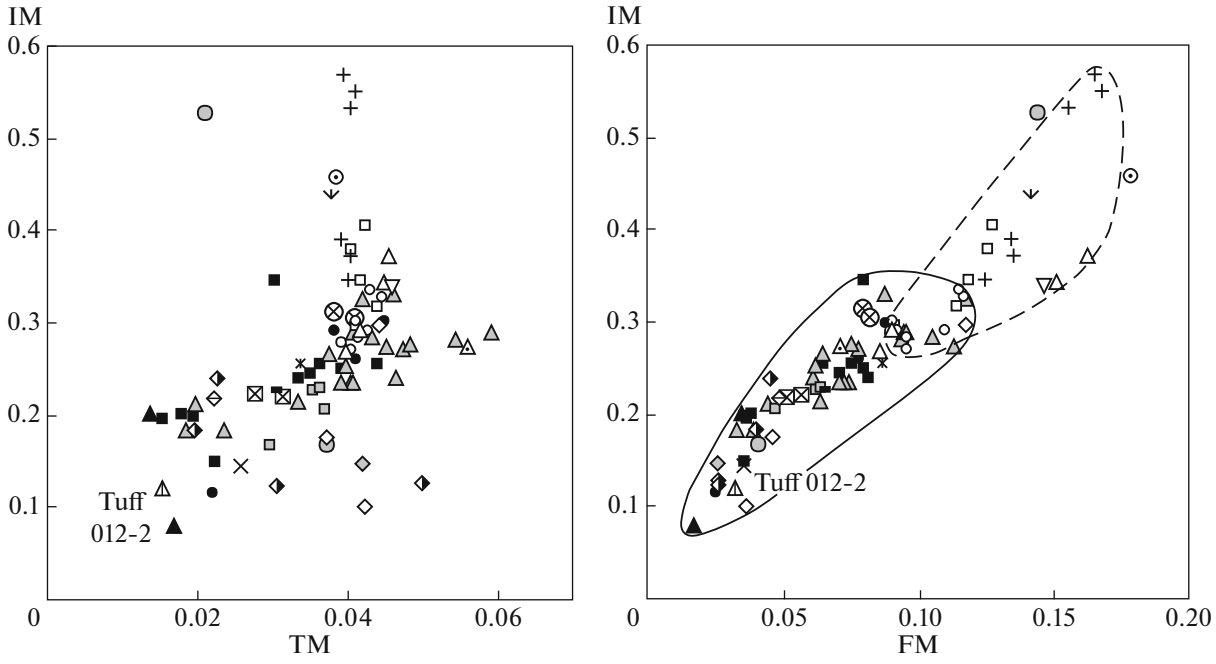

Fig. 6. Module diagrams for Jurassic–Lower Cretaceous rocks of the Bureya basin. For legend, see Figs. 4 and 5.

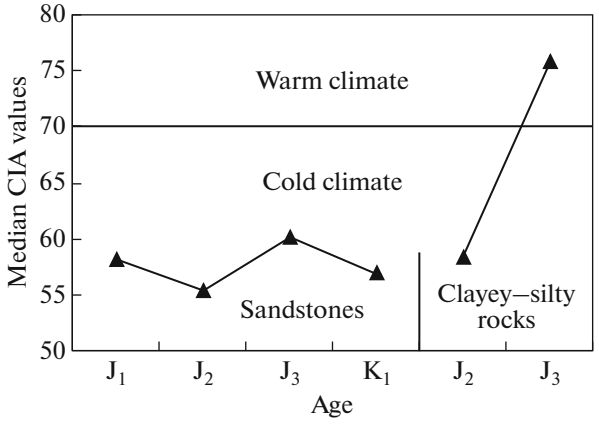

Fig. 7. Plot of changes in the climatic index (CIA) values in Jurassic–Lower Cretaceous rocks of the Bureya basin.

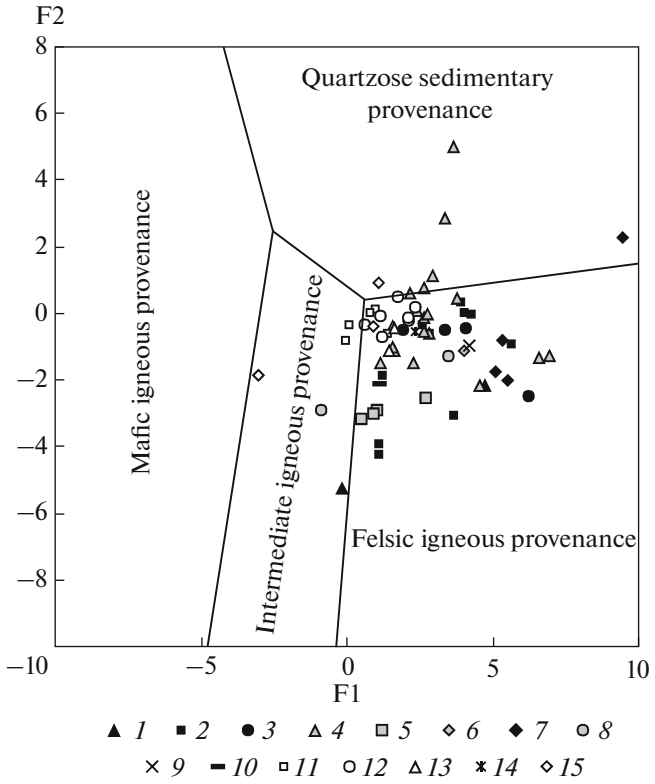

Fig. 8. Position of data points of Jurassic–Lower Cretaceous rocks from the Bureya basin in the diagram of rock composition in provenances, after [26]. (*1–10*) sandstones of formations: (*1*) Desh, (*2*) Sinkal'ta, (*3*) Epikan, (*4*) El'ga, (*5*) Chaganyi, (*6*) Talyndzhan, (*7*) Dublikan, (*8*) Soloni, (*9*) Chagdamyn, (*10*) Chemchuko; (*11–15*) calcareous sandstones of formations: (*11*) Sinkal'ta, (*12*) Epikan, (*13*) Chaganyi, (*14*) Talyndzhan, (*15*) Dublikan. (F1) = $30.638TiO_2/Al_2O_3 - 12.541Fe_2O_3(tot)/Al_2O_3 + 7.329MgO/Al_2O_3 + 12.031Na_2O/Al_2O_3 + 35.402K_2O/Al_2O_3 - 6.382$. F2 = $56.500TiO_2/Al_2O_3 - 10.879Fe_2O_3(tot)/Al_2O_3 + 30.875MgO/Al_2O_3 - 5.404Na_2O/Al_2O_3 + 11.112K_2O/Al_2O_3 - 3.89$.

(Fig. 8). Some data points of sandstones are localized in the field of quartz-enriched sedimentary rocks. A common provenance (with some local variations) is also assumed from the lithochemical characteristics of clusters II–V (sandstones) and clusters VII–IX (clayey–silty rocks), which are similar in every rock type.

Proceeding from the geological situation, the probable provenances could be located west, southwest (Bureya massif as a constituent of the Jiamusi–Khanka–Bureya superterrane), north (Amur–Okhotsk and Stanovik–Dzhugdzhur regions), and east (presumably, Chegdomyn inlier of the Bureya massif) of the region under consideration. In the scope of this investigation, the median chemical compositions of the Jurassic rocks of the Bureya basin were compared with the compositions of the Paleozoic granitoids located immediately westward [3, 14], the pre-Mesozoic intrusive rocks of the Bureya massif as a whole [4], the Amur–Okhotsk domain [4], and the Stanovik–Dzhugdzhur region [4].

In SiO_2, Fe_2O_3, Na_2O, and K_2O, the Jurassic terrigenous rocks are most similar to the closely spaced Paleozoic granitoids of the Bureya massif (Fig. 9). It may confidently be concluded that the main share of detrital material was transported from the west and southwest. It originated most likely from the Bureya massif, which is composed of metamorphic and sedimentary terrigenous rocks, in addition to igneous varieties. This assumption is consistent with the inferences in [6, 8]. It is conceivable that beginning from the Bajocian, some material was transported from the east [6].

It is undoubted that the sedimentation basin received acid material. Its diagnostics in the terrigenous rocks on the basis of oxide contents and lithochemical modules is not a simple task [19, 21]. This is aggravated by the fact that magmatites (intrusive and volcanic) and granite gneisses, also acid in composition and, consequently, bearing similar lithochemical modules, were simultaneously eroded. This task may be solved using the petrographic approach, since peculiar clasts of volcanic glass observable under a microscope in sandstones serve as good indicators of ashes ([20] and others). The presence of intercalations of volcanic rocks and bentonite clays is a reliable indicator of volcanic activity. The analysis of geological maps ([22] and others) allows an assumption that volcanoes may have been located to the north, south, and southwest during different periods, which was noted by previous researchers [5, 6, 9].

In the Jurassic Period, they may be represented by volcanoes in China (present-day coordinates) to the south and southwest and volcanoes of the Uda–Murgal volcanic arc to the north. In the Cretaceous, the Khingan–Olonoi and Ogodzha volcanic belts were active to the west and north, respectively. It is conceiv-

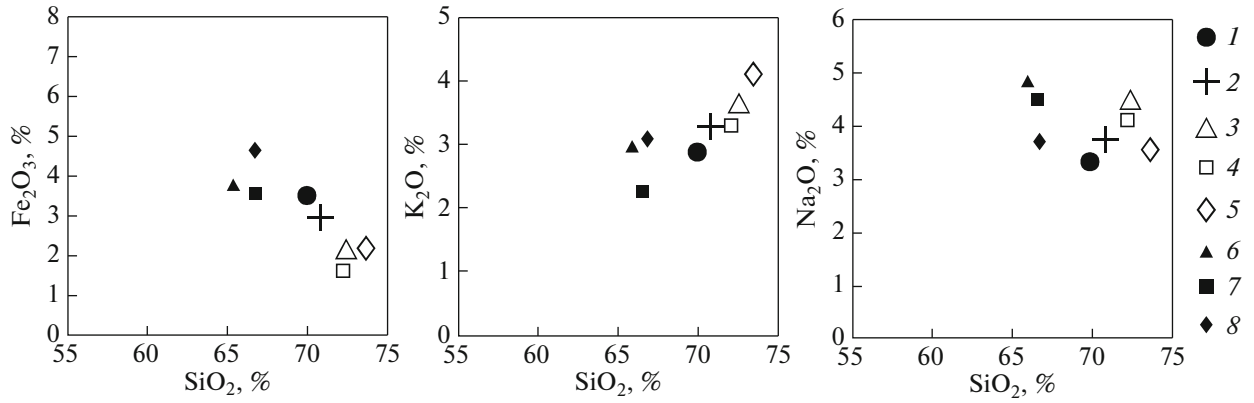

Fig. 9. Position of sandstones from the Bureya basin and pre-Mesozoic intrusive rocks in variation diagrams. (*1*) sandstones; (*2*) Bureya Paleozoic granite, after [3, 14]; (*3–8*) pre-Mesozoic intrusive rocks, after [4]: (*3–5*) granites ((*3*) Stanovik–Dzhugdzhur domain (SDD), (*4*) Amur–Okhotsk domain (AOD), (*5*) Bureya massif as a whole (BM)); (*6–8*) granodiorites ((*6*) SDD, (*7*) AOD, (*8*) BM).

able that the finest fractions may have originated from the volcanoes of the Okhotsk–Chukotka volcanic belt (OCHVB). The share of ash admixture varied depending on the remoteness of the volcanoes, as well as the directions and strength of winds in the Middle–Jurassic and Early Cretaceous epochs. This intriguing problem requires a special investigation.

CONCLUSIONS

(1) In their chemistry, the examined sandstones are of acid composition corresponding to that of the granite–rhyolite series; clayey–silty rocks are transitional between granodiorites and diorites (or their volcanic analogs: dacites and andesites).

(2) The distribution of elements in the clayey–silty rocks is similar to that in the sandstones, which is easily explained by their co-occurrence in alternating sequences.

(3) The Migdisov regularity is not observed.

(4) On the whole, the examined rocks are immature, representing a product of the first sedimentation cycle.

(5) The parent rocks are mostly represented by acid and subordinate intermediate intrusive and volcanic partly metamorphosed rocks (granite gneisses, crystalline schists) and terrigenous sedimentary varieties.

(6) The lithochemical modules give reason to assume the presence of ash admixture in the rocks and to discriminate between acid tuffs, on the one hand, and sandstones (with some conditionality) and clayey–silty rocks (confidently), on the other. In the situation under consideration, diagnostics of the petrogenic and pyrogenic constituents is substantially hampered by the occurrence of rocks within thick sequences of the marginal trough and lithochemical criteria alone are insufficient for their discrimination.

(7) The Bureya massif was the most probable source of clastic material. Its main share was transported from the west and southwest; a smaller share originated from the Chegdomyn inlier located to the east, which is also composed of acid rocks. Ashy material may have been transported from volcanoes located to the south, southwest, and north.

(8) Despite the significant compositional similarity of the examined sedimentary rocks to the rocks in the provenances, more reliable inferences on the position of particular provenances are possible after additional investigations.

ACKNOWLEDGMENTS

I thank G.L. Kirillova, L.F. Mishin, Ya.E. Yudovich and A. I. Malinovsky for consultation, remarks, and recommendations, which were useful for improvement of the manuscript. I am also grateful to T.L. Karpova, L.V. Yakhno, and G.M. Vykhovanets for their help in preparing illustrations and V.G. Klychkova for her help in compiling tables.

This work was supported by the Far East Branch of the Russian Academy of Sciences (project no. 15-I-2-027 "Tectono-sedimentary models of sedimentary basins of southeastern Russia").

REFERENCES

1. V. I. Anoikin, *State Geological Map of the Russian Federation. 1 : 200000. 2nd ed. Bureinskaya Series. Sheet M-53-VIII (Chegdomyn). Explanatory Notes* (VSEGEI, St. Petersburg, 2003) [in Russian].
2. *Atlas of the Mesozoic Marine Fauna of the Russian Far East,* Ed. by I. I. Sei, T. M. Okuneva, T. D. Zonova, and E. A. Kalacheva (VSEGEI, St. Petersburg, 2004) [in Russian].
3. S. M. Braginskii, *Geological Map of the USSR. 1 : 200000. Khingan–Bureinskaya Series, Sheet M-52-VII.*

Explanatory Notes (Nedra, Moscow, 1965) [in Russian].

4. B. I. Burde and N. S. Kravchenko, *Method of Petrochemical Characteristics Based on Deviation from the Model Composition and Petrochemical Features of the Amur Region* (Dal'nauka, Vladivostok, 2003) [in Russian].
5. T. N. Davydova and Ts. L. Gol'dshtein, *Lithological Studies in the Bureya Basin* (Gostoptekhizdat, Moscow, 1949) [in Russian].
6. V. Yu. Zabrodin, "Paleogeography of the Bureya foredeep (in the Far East) in the Jurassic," Russ. J. Pac. Geol. **1** (5), 473–481 (2007).
7. G. L. Kirillova and V. V. Krapiventseva, "Mesocyclicity of Upper Triassic–Jurassic rocks in the Bureya Basin in the Far East of Russia: their tectonics, eustasy, and sequence stratigraphy," Russ. J. Pac. Geol. **6** (4), 294–309 (2012).
8. G. L. Kirillova, "Reconstruction of Late Mesozoic provenances for the East Asian continental margin based on U–Pb detrital zircon geochronology," Dokl. Earth Sci. **456** (2), 646–648 (2014).
9. V. V. Krapiventseva, *Coaliferous Formation of the Bureya Basin* (Nauka, Moscow, 1979) [in Russian].
10. S. A. Medvedeva, "Lithochemical characteristics of Mesozoic terrigenous rocks of the Bureya sedimentary basin," in *Tectobics, Deep Structure, and Metallogeny of East Asia. Proceedings of All-Russian All-Russian Conference of the 8th Kosygin Readings, Khabarovsk, Russia, 2013,* Ed. by A. N. Didenko and Yu. F. Manilov (Dal'nauka, Vladivostok, 2013), pp. 535–538 [in Russian].
11. S. A. Medvedeva, "Mesozoic sandstones and the reconstruction of tectonic depositional environments in the Bureya sedimentary basin in the Far East," Russ. J. Pac. Geol. **8** (4), 300–313 (2014).
12. Pettijohn, F.J., Potter, R., and Siever, R., *Sand and Sandstone* (Springer, Heidelberg, 1972).
13. I. I. Sei and E. D. Kalacheva, *Biostratigraphy of the Lower and Middle Jurassic Sediments of Far East* (Nedra, Leningrad, 1980) [in Russian].
14. V. F. Sigov, *Geological Map of the USSR. 1 : 200000. Khingan–Bureinskaya Series. Sheet M-53-II. Explanatory Notes* (Nedra, Moscow, 1965) [in Russian].
15. *Systematics and Classification of Sedimentary Rocks and Their Analogues,* Ed. by V. N. Shvanov, V. T. Frolov, E. I. Sergeev (Nedra, St. Petersburg, 1998) [in Russian].
16. I. I. Sharudo, V. I. Moskvin, and O. A. Dzens-Litovskaya, *Lithology and Paleogeography of the Bureya Basin in the Late Mesozoic* (Nauka, Novosibirsk, 1973) [in Russian].
17. V. N. Shvanov, *Petrography of Sedimentary Rocks* (Nedra, Leningrad, 1987) [in Russian].
18. V. D. Shutov, "Classification of sandstones," Litol. Polezn. Iskop., No. 5, 86–103 (1967).
19. Ya. E. Yudovich and M. P. Ketris, *Principles of Lithochemistry* (Nauka, St. Petersburg, 2000) [in Russian].
20. Ya. E. Yudovich and M. P. Ketris, *Mineral Indicators of Lithogenesis* (Geoprint, Syktyvkar, 2008) [in Russian].
21. Ya. E. Yudovich and M. P. Ketris, *Geochemical and Mineralogical Indicators of Volcanogenic Products in Sedimentary Sequences* (UrO RAN, Yekaterinburg, 2010) [in Russian].
22. *Geological Map of Amur Region and Adjacent Areas. (Fragment of Sheet 2). 1 : 2500000* (VSEGEI–Amurgeolkom–Mingeo KNR, St. Petersburg, 1998) [in Russian].
23. L. Harnois, "The CIW index: a new chemical index of weathering," Sediment. Geol. **55**, 319–322 (1988).
24. M. M. Herron, "Geochemical classification of terrigenous sand and shales from core or log data," J. Sediment. Petrol. **58** (5), 820–829 (1988).
25. H. W. Nesbitt and G. M. Young, "Early Proterozoic climates and plate motions inferred from major element chemistry of lutites," Nature **299**, 715–717 (1982).
26. B. P. Roser and R. J. Korsch, "Provenance signatures of sandstone-mudstone suites determined using discriminant function analysis of major element data," Chem. Geol. **67**, 119–139 (1988).
27. I. N. J. Visser and G. M. Young, "Major element geochemistry and paleoclimatology of the Permo–Carboniferous Glacigene Dwyka Formation and post-glacial mudrocks in Southern Africa," Paleogeogr., Paleoclimatol., Paleoecol. **81**, 49–57 (1990).

Recommended for publishing by A.V. Koloskov

Translated by I. Basov